Title

Shifts in the Fundamental Frequency of a Fluid Conveying Pipe Immersed in a Viscous Fluid for use in the Optimization of an Energy Harvesting System to be Deployed in a Producing Hydrocarbon Well

Authors

Kjolsing, E
Todd, M

Publication Date

2015-04-27

DOI

10.2118/174047-ms

Peer reviewed

SPE-SPE-174047-MS-MS

Shifts in the Fundamental Frequency of a Fluid Conveying Pipe Immersed in a Viscous Fluid for use in the Optimization of an Energy Harvesting System to be Deployed in a Producing Hydrocarbon Well

E. Kjolsing, and M. Todd, University of California - San Diego

This paper was prepared for presentation at the SPE Western Regional Meeting held in Garden Grove, California, USA, 27–30 April 2015.

Abstract

Novel methods for harvesting energy in down hole applications are desired. Specifically, it is hoped that sufficient power can be generated near a hydrocarbon reservoir to operate commercially available well monitoring equipment. Vibration based harvesters are the most likely systems to be developed. The efficiency of such harvesters is highly dependent on the natural frequency of the structural system. To optimize the harvester design, the dynamic properties of the down hole system must be characterized.

This paper presents the results of an analytical frequency study undertaken to identify the role axial force effects, annulus fluid geometry, and annulus fluid properties have on the first natural frequency of a production string as the conveyed fluid velocity was varied. The system was modeled using an Euler-Bernoulli formulation and includes a hydrodynamic forcing function to account for annulus fluid effects. The problem was solved in the frequency domain using the spectral element method, which conveniently provides natural frequency information.

The results of the study are in-line with previously published studies on analogous systems. It was found that the well annulus geometry, annulus fluid density, and annulus fluid viscosity have a strong role in determining the behavior of the system. Additionally, the axial force, added mass, and viscous effects were found to shift the natural frequency of the system while only axial force and viscous effects cause a shift in the fluid velocity at which bifurcation occurs. These findings, along with the method outlined in this paper, provide a useful tool in the characterization of hydrocarbon producing wells which is a first step towards developing an energy harvesting system.

Although the problem of determining the dynamics of a fluid conveying pipe immersed in a viscous fluid has been approached using a shell formulation in the past, to the authors knowledge this is the first time the problem has been solved with a beam formulation.

Approved for publication, LA-UR-XX-XXXXX. Copyright for this paper have been transferred to SPE.

Introduction

Novel energy harvesters are sought to power down hole production well monitoring systems that, when used in conjunction with commercially available telemetry systems, eliminate the need for running conductor cable within a well annulus. Utilizing the mechanical vibrations stemming from the kinetic

energy of the produced fluid appears to be a common strategy (Schultz et al. 2004; Fripp and Michael 2007; Wetzel et al. 2009; Guerrero et al. 2011; Pabon and Bettin 2013) where the energy harvester is structurally supported by the production string. The energy generated from this strategy is highly sensitive to the frequencies found in the structural system: the harvester needs to be tuned to the natural frequencies of the production string in order to maximize the energy harvested. If the harvester is "out-of-tune," a sufficient amount of energy may not be collected resulting in the monitoring systems being under-powered.

The first step towards the optimal design of an energy harvesting system, then, is to understand the dynamics of the production string. While previous work has investigated the behavior of pipes conveying fluid (Housner 1952; Long 1955; Dodds and Runyan 1965; Naguleswaran and Williams 1968; Paidoussis and Issid 1974; Lee et al. 1995; Lee and Chung 2002; Seo et al. 2005; Lee and Park 2006), these studies failed to account for external mediums such as the confined fluid found in the well annulus. Other studies incorporating external mediums, specifically viscoeleastic foundations (Lottati and Kornecki 1986; Lee et al. 2009; Soltani et al. 2010; Hosseini et al. 2014), do not account for inertial changes known to exist as a beam vibrates in a fluid (Tuck 1969; Yeh and Chen 1978; Siniavskii et al. 1980).

This paper presents the results from a parametric study which investigated the effects of axial force, annulus fluid, and annulus geometry on the first natural frequency of a production string as the conveyed fluid velocity was varied. The problem was formulated using Eurler-Bernoulli beam theory and solved in the frequency domain using the spectral element method (SEM). The results provide insight into the change in dynamic behavior of the production string for various conditions, information useful for the future design and optimization of down hole energy harvesters.

Statement of Theory and Definitions

Hydrocarbon wells are individually designed in order to optimize hydrocarbon extraction. This leads to a variety of potential well configurations. In order to understand the effects of the noted variables of interest, a handful of specific configurations are investigated and compared in a parametric study. To permit a computationally feasible study several idealizations and assumptions are made (see Figure 1):

- The energy harvester is located adjacent to the in-line components the harvester is intended to power.
- The length of production string containing the energy harvester is braced against the production casing to prevent amplified vibrations from damaging adjacent components.
- The bracing elements generate a fixed-fixed boundary condition.
- The production casing is rigid and coaxial to the production string (the production string being centered in the casing by the bracing elements).
- The annulus fluid is single-phase and stagnant.
- The production string has a constant cross section with the tube coupling elements providing negligible changes to the systems mass and stiffness.
- The produced fluid is turbulent and is modeled as plug flow (since the primary interest of this paper is the effects the annulus geometry and annulus fluid have on the system, modeling multiphase flow is considered unnecessarily burdensome).

With these assumptions in mind, the governing equation of motion can be defined. Assuming steady fluid flow and neglecting gravity induced tension effects, the linearized equation of motion for a pipe conveying fluid (Paidoussis and Issid 1974) can be modified to include annulus fluid effects as

$$E^*I\dot{w}'''' + EIw'''' + \{M_iU^2 - \bar{T} + \bar{p}A_i(1-2\nu)\}w'' + 2M_iU\dot{w}' + (M_i+m)gw' + c\dot{w} + (M_i+m)\ddot{w}$$

$$+i\rho_e\pi r_p^2\omega\Gamma U_0 e^{i\omega t} = 0, \quad \text{(1)}$$

where the terms represented are: Kelvin-Voigt dissipation, flexural restoring force, centrifugal force, applied tension, pressure induced tension, Coriolis force, gravity, viscous damping, inertia, and the hydrodynamic force stemming from the annulus fluid. Within equation (1), prime and dot indicate a derivative with respect to spatial location and time, respectively.

The hydrodynamic force (the last term in equation (1)) has been derived by Wamsganss et al. (1974) with similar derivations by Stokes (1851) and Rosenhead (1963). The complex hydrodynamic function, Γ, is defined in Appendix A and contributes both an added mass (a function of $Re[\Gamma]$) and a viscous drag (a function of $Im[\Gamma]$) term to the system through the hydrodynamic force. These effects act to alter the natural frequency of the system and are of particular interest in the present study.

Since both the hydrodynamic function and hydrodynamic force are frequency dependent, equation (1) is solved in the frequency domain using the SEM. A description of the method can be found in the literature (Doyle 1989; Lee 2009) and is not presented here.

Presentation of Data and Results

The results from a parametric study are presented in the following sections: the effects of axial force, annulus fluid density, annulus fluid viscosity, and annulus geometry on the systems first natural frequency were investigated as the conveyed fluid velocity was increased. Note that the negative convention of the fluid velocity used in the following results indicates that the fluid is flowing in the direction opposite gravity, e.g. from the reservoir to the ground surface. The numeric inputs used in the study (see Table 1) are thought to be reasonable but are not intended to represent any specific condition found in practice. Where possible, the results are presented using a normalized conveyed fluid velocity,

$$u = \sqrt{\frac{M_i}{EI}} UL, \quad (2)$$

and a normalized natural frequency

$$\Omega = \sqrt{\frac{M_i+m}{EI}} \omega L^2. \quad (3)$$

Axial Force.

A single system is subject to three different axial loads (cases I-III respectively): 150kN tension, 0kN (e.g. unloaded), and 250kN compression. The change in the first natural frequency for these three cases as the fluid velocity is increased is presented in Figure 2. Note that $Re[\Omega]$ decreases as the fluid velocity increases. This is due to an increasing compression in the system stemming from the centrifugal force generated by the conveyed fluid. Upon revisiting equation 1, specifically the third and fourth terms, the applied axial force is seen to be proportional to the conveyed fluid velocity squared: as the fluid velocity increases, the compression in the system increses. As the compression in the system approaches the Euler buckling load both $Re[\Omega]$ and $Im[\Omega]$ approach zero and divergence instability is reached. For the unloaded system this occurs at a normalized fluid velocity of -6.28 and is in agreement with published results (Rao 2007). For cases I and III, the Euler load can be written as $P_{Euler} = M_i U_{cr}^2 - \bar{T}$ allowing the critical fluid velocities to be calculated as $u_{cr-case\ I} = -6.69$ and $u_{cr-case\ III} = -5.54$. Both results agree well with the results produced by the SEM model shown in Figure 2.

The difference in $Re[\Omega]$ between the three cases for zero flow ($u = 0$) can also be estimated analytically. Using case III as an example, Bolotin (1964) suggested the relationship $\Omega_c = \Omega\sqrt{1 + \bar{T}/P_{Euler}}$ where Ω for the unloaded case was found by the SEM model to be 22.37, agreeing with published results (Paidoussis 1998). Noting $P_{Euler} = 1123.9kN$ for the system, the predicted natural frequency of $\Omega_c = 19.73$ agrees well with the SEM result of 19.80 (error = 0.3%).

Annulus Fluid Density.

Appearing in the definition of the hydrodynamic force, the annulus fluid density acts to scale the effect of the hydrodynamic function. Its effect is illustrated with four inviscid cases (cases IV-VII) shown in Table 2. For each case, real values of the hydrodynamic function are assumed and the conveyed fluid is assumed to be stagnant. Since the real part of the hydrodynamic function contributes only an added mass effect, an analytical calculation of each systems first natural frequency can be made and compared directly with the SEM results.

For each case, the system mass $(M_i + m)$ is known and the added mass can be calculated as $\rho_e \pi r_p^2 Re[\Gamma]$. To analytically determine the natural frequency of the four cases the system stiffness is required. For case IV, the annulus fluid density is taken to be zero resulting in the elimination of the hydrodynamic forcing term from the equation of motion and simplifying the system to a beam vibrating in a vacuum. The natural frequency in this case is widely known to be $\Omega = 22.37$. The stiffness of case IV (and in fact all four cases) can then be calculated as $K = \omega_n^2(M_i + m) = 222696\ kg/ms^2$. Excellent agreement is seen between the analytically calculated and the SEM model estimates of the natural frequencies for the four cases shown in Table 2

Annulus Viscosity and Geometry.

The hydrodynamic force is dependent on the hydrodynamic function, itself dependent on the annulus fluid viscosity and annulus geometry, as shown in Appendix A. The relationship between the three inputs (υ_e, r_c, r_p) and the resulting hydrodynamic function is not transparent. The next section investigates how these three variables work to define the hydrodynamic function while the two sections that follow investigate how the hydrodynamic function affects the natural frequency of inviscid and viscous systems.

Hydrodynamic Function.

Four hydrodynamic functions are defined by the inputs listed in Table 3 with the real and imaginary parts of the resulting hydrodynamic functions plotted in Figure 3. Recall that the real part of the hydrodynamic function generates an added mass in the system while the imaginary part generates a viscous drag. The following can be observed for the the inputs considered:

- $Re[\Gamma]$ and $|Im[\Gamma]|$ increase with a decreasing r_c/r_p ratio.
- $Re[\Gamma]$ and $|Im[\Gamma]|$ increase with an increasing annulus fluid viscosity.

Inviscid System.

Cases IX and X assume an inviscid annulus fluid with varying annulus geometry (case VIII acts as the benchmark beam in vacuum case). The natural frequencies are plotted in Figure 4 as the conveyed fluid velocity is increased. As the casing radius (r_c) is decreased (e.g. moving from case IX to X), the real part of the hydrodynamic function increases (an inviscid annulus fluid leads to a purely real hydrodynamic function) resulting in an increased system mass and a decrease in the systems natural frequency. The shifts in $Re[\Gamma]$ for $u = 0$ can be calculated analytically as was done in the *Annulus Fluid Density* section. The results of the analytical calculation can be found in Table 4 and are in agreement with the SEM results.

Returning to Figure 4, divergence instability is seen to occur at $u_{cr} = -6.28$ for all three cases. Since divergence is a static phenomenon, its occurance is not dependent on inertial effects generated by the inviscid annulus fluid.

Viscous System.

Cases XII-XIV assume a viscous annulus fluid with varying annulus geometry and annulus fluid viscosity (case XI, again, acts as a beam in vacuum benchmark). Unlike the inviscid systems, the vertical shift in the real part of the natural frequency is now attributable to both added mass (stemming

from $Re[\Gamma]$) and viscous drag (stemming from $Im[\Gamma]$). This difference is apparent when comparing cases XII and XIII when $u = 0$. The added mass in case XII is much greater than that of case XIII, which if no other hydrodynamic effect existed would have resulted in $Re[\Omega]_{case\ XII} < Re[\Omega]_{case\ XIII}$. However, since the the viscous drag associated with case XIII is much larger than that of case XII the combined effect of the viscous fluid is $Re[\Omega]_{case\ XII} > Re[\Omega]_{case\ XIII}$ as seen in Figure 5.

Bifurcation occurs when the real part of the natural frequency reaches zero. Once bifurcation is reached, the system behaves in an overdamped manner. The bifurcation point of cases XI-XIV differ due to the different levels of viscous drag in each case. If the conveyed fluid velocity is increased past the bifurcation point, the complex natural frequency of the system will continue to migrate towards the point of divergence ($Re[\Omega] = Im[\Omega] = 0$); the system becomes unstable once divergence is reached. Note that like the inviscid cases the divergence point for cases XI-XIV all coincide: divergence is a static phenomenon and is not dependent on added mass or damping.

Conclusions

A parametric study was performed to investigate the effect axial force, annulus fluid properties, and annulus geometry had on the natural frequency of a braced length of production string. The study was motivated by the desire to develop an optimized down hole energy harvester that will be structurally supported by the production string. The results of the study are in agreement with previous studies of analogous systems and are as follows:

- Axial force acts to alter the stiffness of the structural system.
- The annulus fluid density scales the effects of the hydrodynamic function.
- The hydrodynamic function contributes added mass and viscous drag through its real and imaginary parts, respectively.
- A shift in the bifurcation point is seen when the annulus fluid is viscous or externally applied axial forces are included in the system.

This study was a first step towards the development of an optimal, mechanically based, down hole energy harvester.

Acknowledgments

Funding was provided by Los Alamos Laboratory through the Engineering Institute under Task 5 (Subcontract No. 77137-001-11).

Nomenclature

Dimensionless Terms

i = imaginary unit
u = normalized fluid velocity
u_{cr} = nondimensional critical fluid velocity
I_0, I_1, K_0, K_1 = modified Bessel functions
$Im[]$ = imaginary part
$Re[]$ = real part
ν = poisson ratio
Γ = hydrodynamic function
Ω = normalized natural frequency
Ω_c = normalized natural frequency adjusted for compression

Dimensional Terms

c = viscous damping coefficient
f_{hydro} = hydrodynamic force

g = coefficient of gravity
m = mass per unit length of pipe
m_{added} = added mass
$\bar{p}$ = mean pressure differential
r_c = confining shell inner radius
r_p = pipe outer radius
t = time
w = lateral deflection of the pipe
w_t = pipe wall thickness
A_i = flow area
A_p = pipe cross sectional area
E = Young's modulus
E^* = Kelvin-Voigt viscosity
I = pipe inertia
K = system stiffness
L = pipe length
M_i = mass per unit length of conveyed fluid
P_{Euler} = Euler buckling load
$\bar{T}$ = externally applied tension
U = mean axial flow
U_{cr} = critical fluid velocity
$U_0 e^{i\omega t}$ = pipe velocity
ρ_e = annulus fluid density
ρ_i = conveyed fluid density
ρ_p = pipe density
υ_e = annulus fluid kinematic viscosity
ω = radial frequency
ω_n = natural frequency

References

1 Bolotin, V. V. 1974. *The dynamic stability of elastic systems*. Holden-Day, Inc.
2 Dodds Jr, H. L. and Runyan, H. L. 1965. Effect of high-velocity fluid flow on the bending vibrations and static divergence of a simply supported pipe. No. NASA-TN-D-2870. National aeronautics and space administration Hampton VA Langley Research Center.
3 Doyle, J. F. 1989. *Wave propagation in structures*. Springer US.
4 Fripp, M. L. and Michael, R. K. 2007. *U.S. Patent No. 7,199,480*. Washington, DC: U.S. Patent and Trademark Office.
5 Guerrero, J. C., Pabon, J. A., Auzerais, F. M., Chen, K. C. and Forbes, K. J. 2011. *U.S. Patent No. 7,906,861*. Washington, DC: U.S. Patent and Trademark Office.
6 Hosseini, M., Sadeghi-Goughari, M., Atashipour, S. A. and Eftekhari, M. (2014). Vibration analysis of single-walled carbon nanotubes conveying nanoflow embedded in a viscoelastic medium using modified nonlocal beam model. *Archives of Mechanics* **66** (4), 217-244.
7 Housner, G. W. 1952. Bending vibrations of a pipe line containing flowing fluid. *Journal of Applied Mechanics-Transactions of the ASME* **19** (2), 205-208.
8 Lee, U. 2009. *Spectral element method in structural dynamics*. John Wiley & Sons.
9 Lee, S. I. and Chung, J. 2002. New non-linear modelling for vibration analysis of a straight pipe conveying fluid. *Journal of Sound and Vibration* **254** (2), 313-325.
10 Lee, U., Jang, I. and Go, H. 2009. Stability and dynamic analysis of oil pipelines by using spectral element method. *Journal of Loss Prevention in the Process Industries* **22** (6), 873-

878.
11 Lee, U., Pak, C. H. and Hong, S. C. 1995. The dynamics of a piping system with internal unsteady flow. *Journal of Sound and Vibration* **180** (2), 297-311.
12 Lee, U., and Park, J. 2006. Spectral element modelling and analysis of a pipeline conveying internal unsteady fluid. *Journal of Fluids and Structures* **22** (2), 273-292.
13 Long, R. H. 1955. Experimental and theoretical study of transverse vibration of a tube containing flowing fluid. *Journal of Applied Mechanics* **77** (1), 65-68.
14 Lottati, I. and Kornecki, A. 1986. The effect of an elastic foundation and of dissipative forces on the stability of fluid-conveying pipes. *Journal of Sound and Vibration* **109** (2), 327-338.
15 Naguleswaran, S. and Williams, C. J. H. 1968. Lateral vibration of a pipe conveying a fluid. *Journal of Mechanical Engineering Science* **10** (3), 228-238.
16 Pabon, J. A. and Bettin, G. 2013. *U.S. Patent No. 8,604,634*. Washington, DC: U.S. Patent and Trademark Office.
17 Paidoussis, M. P. 1998. *Fluid-structure interactions: slender structures and axial flow. Vol. 1*. Academic Press.
18 Paidoussis, M. P. and Issid, N. T. 1974. Dynamic stability of pipes conveying fluid. *Journal of Sound and Vibration* **33** (3), 267-294.
19 Rao, S. S. 2007. *Vibration of continuous systems*. John Wiley & Sons.
20 Rosenhead, L. 1963. *Laminar Boundary Layers*. Oxford: Clarendon Press.
21 Schultz, R. L., Michael, R. K., Robison, C. E. and Ringgenberg, P. D. 2004.*U.S. Patent No. 6,768,214*. Washington, DC: U.S. Patent and Trademark Office.
22 Seo, Y. S., Jeong, W.B., Jeong, S. H., Oh, J. S. and Yoo, W. S. 2005. Finite element analysis of forced vibration for a pipe conveying harmonically pulsating fluid. *JSME International Journal Series C* **48** (4), 688-694.
23 Siniavskii, V. F., Fedotovskii, V. S. and Kukhtin, A. B. 1980. Oscillation of a Cylinder in a Viscous Liquid. *Prikladnaia Mekhanika* **16**, 62-67.
24 Soltani, P., Taherian, M. M., and Farshidianfar, A. 2010. Vibration and instability of a viscous-fluid-conveying single-walled carbon nanotube embedded in a visco-elastic medium. *Journal of Physics D: Applied Physics* **43** (42), 425401.
25 Stokes, G. G. 1851. *On the effect of the internal friction of fluids on the motion of pendulums. Vol. 9.* Pitt Press.
26 Tuck, E. O. 1969. Calculation of unsteady flows due to small motions of cylinders in a viscous fluid. *Journal of Engineering Mathematics* **3** (1), 29-44.
27 Wambsganss, M. W., Chen, S. S. and Jendrzejczyk, J. A. 1974. Added mass and damping of a vibrating rod in confined viscous fluids. NASA STI/Recon Technical Report N 75, 10349.
28 Wetzel, R. J., Hiron, S., Veneruso, A. F., Patel, D. R., MacDougall, T. D. and Walter, J. 2009. *U.S. Patent Application 12/400,024*.
29 Yeh, T. T. and Chen, S. S. 1978. The effect of fluid viscosity on coupled tube/fluid vibrations. *Journal of Sound and Vibration* **59** (3), 453-467.

Conversions

m	x 3.28 E0	$= ft$
$\boldsymbol{m^2}$	x 1.08 E1	$= \boldsymbol{ft^2}$
$\boldsymbol{m^4}$	x 1.16 E2	$= \boldsymbol{ft^4}$
m/s	x 3.28 E0	$= ft/s$
m/s^2	x 3.28 E0	$= ft/s^2$
m^2/s	x 1.08 E1	$= ft^2/s$
kg/m	x 6.72 E-1	$= lb/ft$
kg/m^3	x 6.24 E-2	$= lb/ft^3$

kg/s	x 2.20 E0	$= lb/s$
kg/ms	x 6.72 E-1	$= lb/fts$
kg/ms^2	x 6.72 E-1	$= lb/fts^2$
N	x 2.25 E-1	$= lb$
N/m^2	x 2.09 E-2	$= lb/ft^2$

Appendix A

To derive the hydrodynamic function, the following assumptions were made:

- The production string has a uniform cross section and is concentric to a rigid cylindrical surface.
- The length between bracing elements greatly exceeds the diameter of the production string.
- The annulus fluid has zero velocity at the outer boundary (e.g. the casing) and a velocity that matches the production string at the pipe-fluid interface.
- Production string displacements are small.
- The annulus fluid is Newtonian, homogeneous, and incompressible.

The hydrodynamic function is then written as

$$\Gamma = \frac{\Gamma_{num}}{\Gamma_{den}} - 1 = Re[\Gamma] - iIm[\Gamma], \quad \text{(A.1)}$$

with the arguments Γ_{num} and Γ_{den} given as

$$\Gamma_{num} = 2\alpha^2[I_0(\alpha)K_0(\beta) - I_0(\beta)K_0(\alpha)] - 4\alpha[I_1(\alpha)K_0(\beta) + I_0(\beta)K_1(\alpha)]$$

$$+4\alpha\gamma[I_0(\alpha)K_1(\beta) + I_1(\beta)K_0(\alpha)] - 8\gamma[I_1(\alpha)K_1(\beta) - I_1(\beta)K_1(\alpha)] \quad \text{(A.2)}$$

and

$$\Gamma_{den} = \alpha^2(1-\gamma^2)[I_0(\alpha)K_0(\beta) - I_0(\beta)K_0(\alpha)]$$

$$+2\alpha\gamma[I_0(\alpha)K_1(\beta) - I_1(\beta)K_0(\beta) + I_1(\beta)K_0(\alpha) - I_0(\beta)K_1(\beta)]$$

$$+2\alpha\gamma^2[I_0(\beta)K_1(\alpha) - I_0(\alpha)K_1(\alpha) + I_1(\alpha)K_0(\beta) - I_1(\alpha)K_0(\alpha)] \quad \text{(A.3)}$$

The arguments to the hydrodynamic function are

$$\gamma = \frac{r_p}{r_c}, \quad \text{(A.4)}$$

$$\bar{k} = \sqrt{\frac{i\omega}{\upsilon_e}}, \quad \text{(A.5)}$$

$$\alpha = \bar{k}r_p, \quad \text{(A.6)}$$

and

$$\beta = \bar{k}r_c. \quad \text{(A.7)}$$

Tables

		Case													
		Axial Force Effects			Annulus Fluid Density				Inviscid System			Viscous System			
Variable	*Units*	I	II	III	IV	V	VI	VII	VIII	IX	X	XI	XII	XIII	XIV
E^*	kg/ms	0			0				0			0			
E	N/m^2	2E+11			2E+11				2E+11			2E+11			
r_p	m	0.065			0.065				0.065			0.065			
w_t	m	0.015			0.015				0.015			0.015			
I	m^4	9.11E-06			9.11E-06				9.11E-06			9.11E-06			
A_p	m^2	5.42E-03			5.42E-03				5.42E-03			5.42E-03			
A_i	m^2	7.85E-03			7.85E-03				7.85E-03			7.85E-03			
ν	-	0			0				0			0			
ρ_p	kg/m^3	7800			7800				7800			7800			
m	kg/m	42.27			42.27				42.27			42.27			
g	m/s^2	9.81			9.81				9.81			9.81			
L	m	8			8				8			8			
ρ_i	kg/m^3	900			900				900			900			
ρ_e	kg/m^3	0			0	2000	600	1200	0	1050		0	1050		
r_c	m	∞			NA**				∞	1.30d	1.11d	∞	1.10d	1.11d	1.10d
v_e	m^2/s	0			NA**				0			0	1.2E-05	1.2E-04	
M_i	kg/m	7.07			7.07				7.07			7.07			
U	m/s	Varies*			0				Varies*			Varies*			
$\bar{T}$	N	1.5E+05	0	-2.5E+05	0				0			0			
$\bar{p}$	N/m^2	0			0				0			0			
c	kg/s	0			0				0			0			

**The flow velocity is taken to be negative, indicating flow in the direction opposite gravity.*

***Hydrodynamic function is hard coded to specified numeric values.*

Table 1 - Parametric study inputs.

Case	Γ	$\rho_e \left(\frac{kg}{m^3}\right)$	$m_{added} \left(\frac{kg}{m}\right)$	Ω	
				Analytical*	SEM
IV	0	0	0.00	22.37	22.37
V	1	2000	26.55	18.04	18.04
VI	2	600	15.93	19.45	19.45
VII	3	1200	47.78	15.95	15.95

* $\Omega = \sqrt{\frac{K(M_i + m)}{EI(M_i + m + m_{added})}} L^2$

Table 2 - Annulus fluid density effects.

		$\frac{r_c}{r_p}$	
		1.1	1.3
$v_e \left(\frac{m^2}{s}\right)$	5E-05	H1	H2
	1E-05	L1	L2

$r_p = 0.065m$

Table 3 - Hydrodynamic function inputs.

Case	Γ	$\rho_e \left(\frac{kg}{m^3}\right)$	$m_{added} \left(\frac{kg}{m}\right)$	Ω	
				Analytical*	SEM
VIII	1.00	0	0.00	22.37	22.37
IX	3.90	1050	54.33	15.44	15.44
X	9.62	1050	134.03	11.61	11.61

$$* \Omega = \sqrt{\frac{K(M_i + m)}{EI(M_i + m + m_{added})}} L^2$$

Table 4 - Added mass effects with zero flow.

Figures

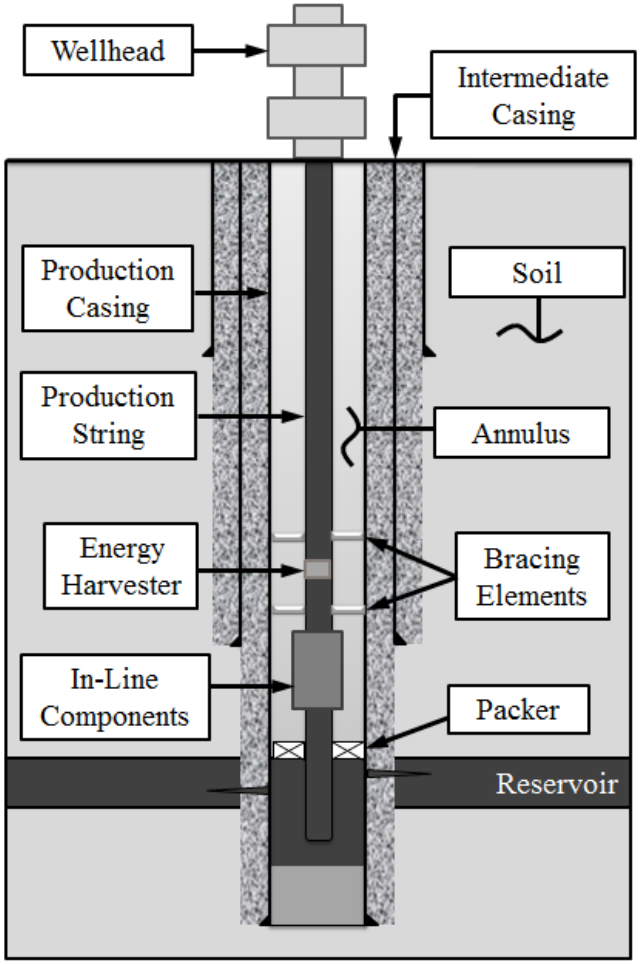

Figure 1 - Well configuration.

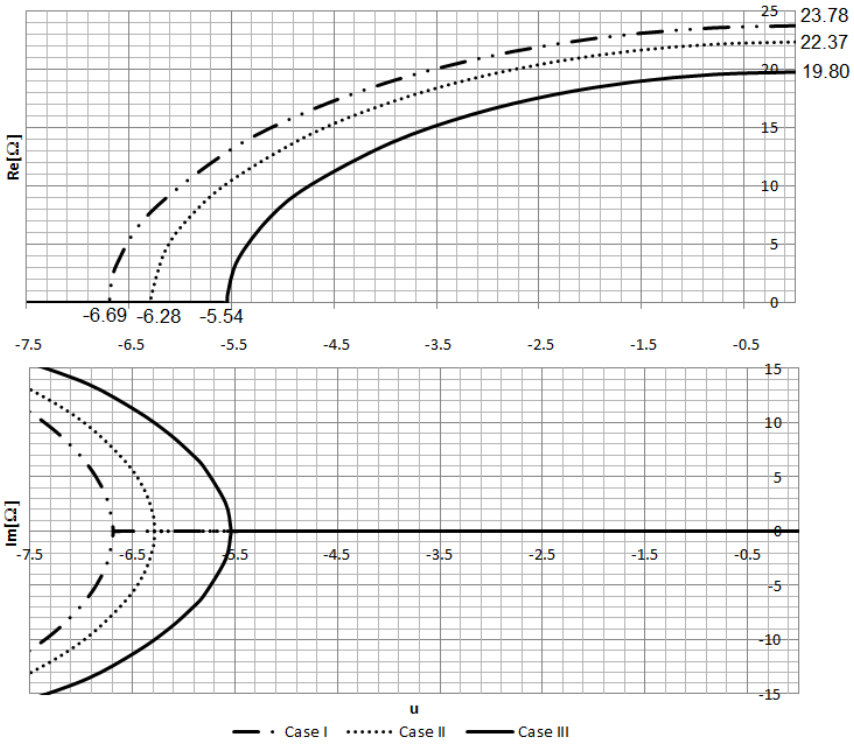

Figure 2 - Axial force effects: flow velocity vs. fundamental frequency.

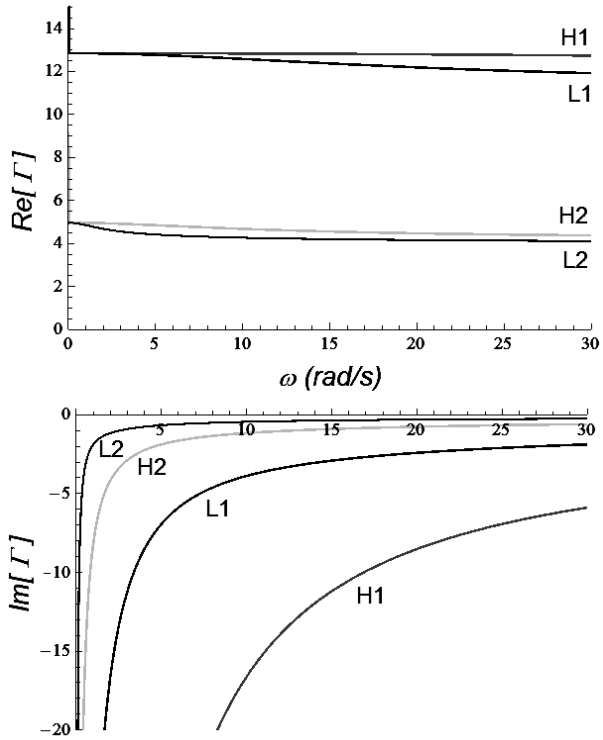

Figure 3 - Hydrodynamic function: real (top) and imaginary (bottom) for various inputs.

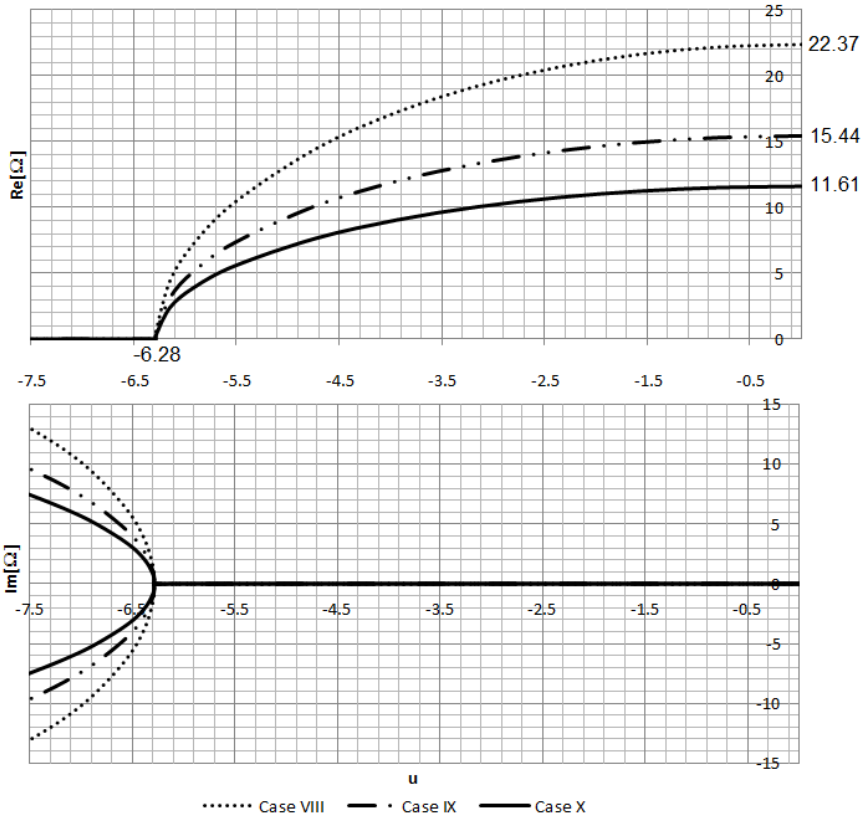

Figure 4 - Inviscid system: flow velocity vs. fundamental frequency.

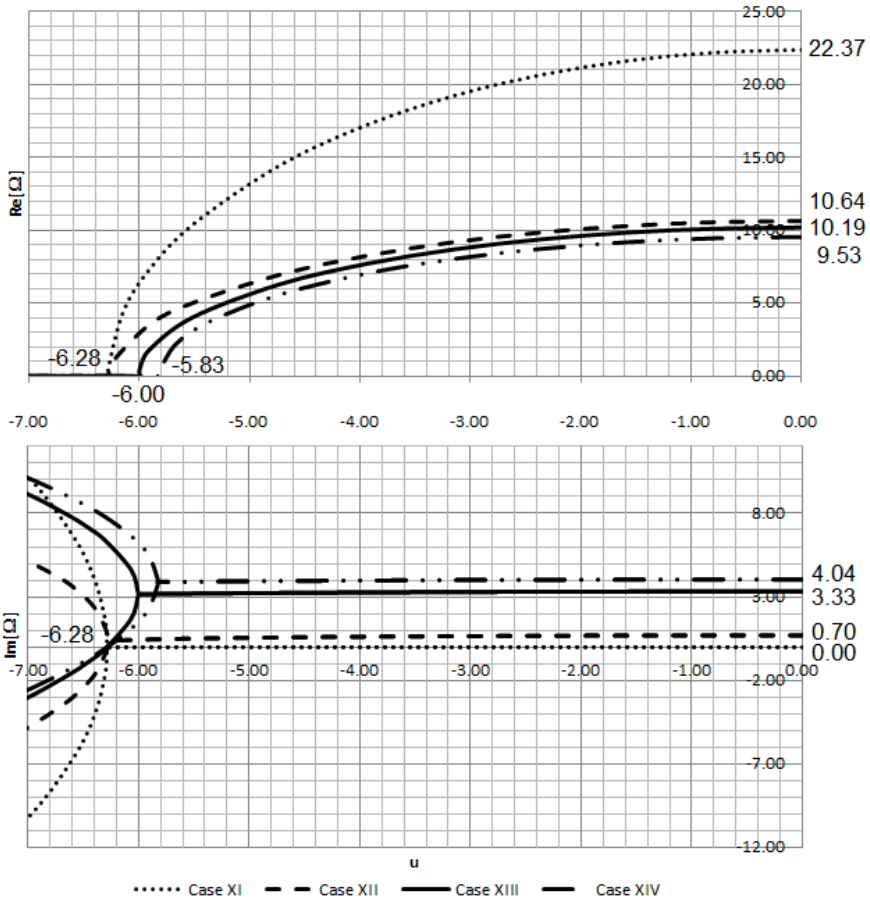

Figure 5 - Viscous system: flow velocity vs. fundamental frequency.